Radiative Hyperon Decays, $\Sigma^{\pm} \rightarrow n+\pi^{\pm}+\gamma$ *

MING CHIANG LI†‡
University of Maryland, College Park, Maryland
(Received 23 August 1965)

The observation of the $\Sigma^{\pm} \rightarrow n+\pi^{\pm}+\gamma$ radiative-decay spectra has been proposed as a method of determining the s- or p-wave nature of the Σ pionic decay. The previous theoretical treatment is based on a phenomenological interaction that neglects all form-factor effects. Calculations have been made to investigate the sensitivity of the theoretical predictions to structure effects by using two models: (a) a self-consistent pole model that includes the $\Sigma^{+} \rightarrow p+\gamma$ vertex in a natural way; (b) a loop model that serves as a demonstration of the radiative influence of a virtual light particle. The results show that the simple phenomenological calculation is not changed significantly. Hence, the reliability of the radiative-decay method to determine the s- or p-wave nature of Σ pionic decay is improved.

I. INTRODUCTION

IT has been shown by Nauenberg, Barshay, and Schultz,[1] and by Li and Snow[2] that a measurement of the branching ratios for radiative Σ decays of the type

$$\Sigma^{+} \rightarrow n+\pi^{\pm}+\gamma \tag{1.1}$$

can determine the s- or p-wave nature of the nonradiative Σ decays:

$$\Sigma^{\pm} \rightarrow n+\pi^{\pm}. \tag{1.2}$$

A phenomenological calculation of the branching ratios for radiative hyperon decays has been made by Barshay and Behrends.[3] These authors evaluated the angular and energy distributions of the decay nucleon from reaction (1.1) and point out the possibility of obtaining information about the Σ^{+} and Σ^{-} magnetic moments from a study of radiative decays with large γ-ray momenta. Since it is the charged pion rather than the neutron or γ ray that is observed in a typical bubble-chamber experiment, the main purpose of the paper is to examine extensively the charged-pion spectra expected in these radiative decays.

The s- or p-wave nature of the nonradiative Σ decays (1.2) is indirectly related to the $\Delta I=\frac{1}{2}$ rule in the weak interaction.[4] The present experimental values of the parameters $\alpha^{\pm}$ which describe the decay angular distributions combined with time reversal invariance and the $\Delta I=\frac{1}{2}$ rule in weak decay require that one of the Σ decays (1.2) proceed via p wave and the other via s wave. It is known presently that time-reversal invariance does not hold generally in the weak interaction. However, even if it is true in the case of the Σ decays (1.2), one can still show that these decays are either pure s or pure p wave if one uses the $\Delta I=\frac{1}{2}$ rule and the asymmetry parameter values $\alpha^{+}=\alpha^{-}=0$, $\alpha^{0}=1$, and the decay rates $\omega^{+}=\omega^{-}=\omega^{0}$.[5]

In Sec. III the pion spectra are studied using the same phenomenological interaction Hamiltonian of Barshay and Behrends.[3] For the differential pion energy spectra for reaction (1.1) we have evaluated rigorous expressions, where the square terms of magnetic moment corrections from the hyperon, $\Sigma^{\pm}$, and neutron, n, are included. In the later discussions the integrated pion energy spectra are evaluated numerically. This phenomenological model only considers contributions to the radiative decays from inner bremsstrahlung. In particular, there are decay processes involving the transition between the hyperon and the nucleon with the emission of photon followed (or preceded) by the strong emission of a pion by a baryon that are not included. Such processes would be related to the decay $\Sigma^{\pm} \rightarrow p+\gamma$. In order to clarify this problem we shall consider more complicated and detailed models.

In Sec. IV the nonradiative Σ decays (1.2) are considered in the pole model.[6] We assume that the (1.2) decay amplitudes are dominated by the Σ, Λ, and N pole-term contributions. That is to say that the decay proceeds through a Yukawa-type strong vertex and a two-fermion effective weak vertex. For the radiative decays, the electromagnetic interactions are introduced in the conventional way for these nonradiative decay structures. In this model the $\Sigma^{+} \rightarrow p+\gamma$ vertex enters in a natural way and the influence of the $\Sigma^{0}(\Lambda) \rightarrow n+\gamma$ vertex is also considered. The expressions for the differential pion energy spectra in this model are quite complicated and were evaluated numerically on the

* Supported in part by the U. S. Atomic Energy Commission.
† Based on part of a dissertation in partial fulfillment of the requirements for a Ph.D. at the University of Maryland, 1965.
‡ Present address: Institute for Advanced Study, Princeton, New Jersey.
[1] U. Nauenberg, S. Barshay, and J. Schultz, Phys. Rev. Letters **12**, 79 (1964).
[2] M. C. Li and G. A. Snow, University of Maryland, Technical Report No. 351, 1964 (unpublished).
[3] S. Barshay and R. E. Behrends, Phys. Rev. **114**, 931 (1959); S. Iwao and J. Leitner, Nuovo Cimento **22**, 904 (1961).
[4] M. Gell-Mann and A. Rosenfeld, Ann. Rev. Nucl. Sci. **7**, 454 (1957).
[5] B. Cork, L. Kerth, W. Wenzel, J. Cronin, and R. Cool, Phys. Rev. **120**, 1000 (1960); E. Beall, B. Cork, D. Keefe, W. Murphy, and W. Wenzel, Phys. Rev. Letters **8**, 75 (1962); R. Tripp, M. Watson, and M. Ferro-Luzzi, *ibid.* **9**, 66 (1962); J. Cronin and O. Overseth, Phys. Rev. **129**, 1795 (1963); C. Batlay, H. Courant, W. Fichinger, E. Fowler, H. Kraybill, J. Sandweiss, J. Sandord, D. Stonehill, and H. Taft, Rev. Mod. Phys. **33**, 374 (1961); F. Crawford Jr., F. Girard, and G. Smith, Phys. Rev. **128**, 368 (1962); P. Franzini, A. Garfinkel, J. Keren, A. Michelini, R. Planel, A. Prodell, M. Schwartz, J. Steinberger, and S. E. Wolf, Bull. Am. Phys. Soc. **5**, 224 (1960); R. Cool, B. Cork, J. Cronin, and W. A. Wenzel, Phys. Rev. **114**, 912 (1959).
[6] G. Feldman, P. T. Matthews, and A. Salam, Phys. Rev. **121**, 302 (1961); S. K. Bose and R. Marshak, Nuovo Cimento, **23**, 556 (1962); A. Fujii, Phys. Letters **1**, 75 (1962); V. Singh and B. M. Udgaonkar, Phys. Rev. **126**, 2248 (1962); J. C. Pati, *ibid.* **130**, 2097 (1963).

Maryland IBM 7094. In the end of Sec. IV the K loop is also taken into account[7] for the nonradiative decays. In the K-loop model structure, a fast pion occurs in an intermediate state, so that an evaluation of these terms may serve as a measure of the electromagnetic influence of a light swift intermediate particle on the radiative pion spectra. In Sec. V the numerical results are given. It shows that the phenomenological model and the Σ, Λ, N pole models give similar results except for the magnetic moment contributions, and the K-loop contribution for the radiative decays can be completely neglected. The results of our calculations serve to support the theoretical arguments of Nauenberg *et al.*[1] that radiative decays can be used to determine the s- or p-wave nature of $\Sigma \to n+\pi$ decays. A comparison of these calculations with experimental results is briefly discussed.

II. $\Sigma^{\pm} \to n+\pi^{\pm}$ DECAYS

For our later convenience we would like to outline some results of the $\Sigma^{\pm} \to n+\pi^{\pm}$ decays based on the following phenomenological Lagrangian:

$$L_{\text{int}} = (g/\mu)\psi_2(ia+b\gamma_5)\gamma^{\nu}\psi_1\partial_{\nu}\varphi^* + \text{H.c.} \quad (2.1)$$

The indices 1 and 2 refer, respectively, to the hyperon and nucleon. $\varphi(\psi)$ is the meson (baryon) field operator; g/μ is the coupling constant. The parameters a and $b(|a|^2+|b|^2=1)$ are a measure of the degree of parity nonconservation for the $\Sigma^{\pm} \to n+\pi^{\pm}$ decays. If $|a|=1$, $|b|=0$, the decay is through s wave (parity nonconserving); if $|a|=0$, $|b|=1$, it is the parity-conserving p-wave decay. The first-order decay amplitude A for $\Sigma^{\pm} \to n+\pi^{\pm}$, illustrated in Fig. 1, can be written down from the well-known Feynman rules:

$$A = -\frac{g}{\mu}(2\pi)^{-1/2}\delta(p_1-p_2-q)\left(\frac{m_1m_2}{E_1E_2 2Q}\right)^{1/2} \times \bar{W}^s(p_2)(ia+b\gamma_5)\gamma^{\nu}q_{\nu}W^r(p_1), \quad (2.2)$$

where $p=(\mathbf{p},E)$ and $q=(\mathbf{q},Q)$ are the four-momenta of the baryon and pion. m and $W(p)$ are the mass and spinor of the baryon. In the rest system of the hyperon the decay transition rate is

$$W = \left(\frac{g}{\mu}\right)^2 \frac{1}{8\pi m_1^2}\left[\left(\frac{m_1^2-m_2^2+\mu^2}{2m_1}\right)^2-\mu^2\right]^{1/2} \times\{|a|^2(m_1-m_2)^2[(m_1+m_2)^2-\mu^2] + |b|^2(m_1+m_2)^2[(m_1-m_2)^2-\mu^2]\}. \quad (2.3)$$

Notice that in Eq. (2.3), the only difference between the a part and the b part is the replacement $m_2 \to -m_2$. This type of relationship between the a part and b part is also true in the later calculations of the $\Sigma^{\pm} \to n+\pi^{\pm}+\gamma$ decays. The reason is simple. In the trace calculation when we try to cancel the two γ_5's in the b part the sign preceding m_2 is automatically changed. This simplifies the calculation in that it is only necessary to calculate one of the two possibilities, s-wave type or p-wave type, and the other is then obtained directly.

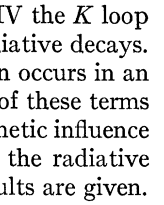

FIG. 1. Feynman diagrams for $\Sigma^{\pm} \to n+\pi^{\pm}$ decays in the phenomenological model.

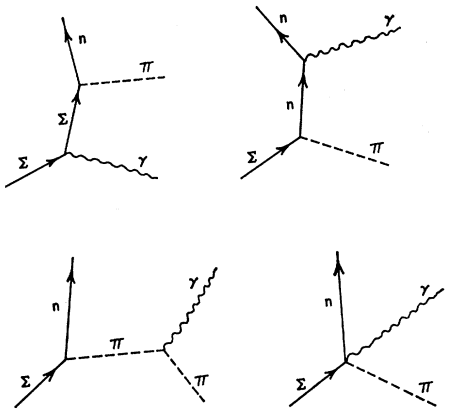

FIG. 2. Feynman diagrams for $\Sigma^{\pm} \to n+\pi^{\pm}+\gamma$ decays in the phenomenological model.

III. $\Sigma^{\pm} \to n+\pi^{\pm}+\gamma$ DECAYS

In this section we deal with a simple model for calculating $\Sigma^{\pm} \to n+\pi^{\pm}+\gamma$ decays. This model suggests that one can determine the s- or p-wave nature of $\Sigma^{\pm} \to n+\pi^{\pm}$ from a study of the momentum spectra of the pions in the $\Sigma^{\pm} \to n+\pi^{\pm}+\gamma$ decays[1,2] whose interaction is taken as

$$L_{\text{int}} = (g/\mu)\bar{\psi}_2(ia+b\gamma_5)\gamma^{\nu}\psi_1(\partial_{\nu}+i\epsilon_3A_{\nu})\varphi^* - \sum_{i=1}^{2}\epsilon_i\bar{\psi}_iA\psi_i - \tfrac{1}{2}\sum_{i=1}^{2}\mu_i\bar{\psi}_i\sigma^{\mu\nu}\psi_iF_{\mu\nu} - i\epsilon_3(\varphi^*\partial_{\mu}\varphi)A^{\mu} + \epsilon_3^2A^{\mu}A_{\mu}\varphi^*\varphi + \text{H.c.}, \quad (3.1)$$

where $F_{\mu\nu}=\partial_{\mu}A_{\nu}-\partial_{\nu}A_{\mu}$, ϵ_1, ϵ_2, and ϵ_3 are the charges of the hyperon, nucleon, and meson, respectively. μ_1 and μ_2 are the static anomalous magnetic moments of the hyperon and nucleon. The interaction (3.1) was originally used by Barshay and Behrends to calculate the nucleon spectra of the same decays. The above interaction is introduced in the customary manner by making the replacement

$$\partial_{\mu}\varphi \to (\partial_{\mu}-i\epsilon_3A_{\mu})\varphi, \qquad \partial_{\mu}\varphi^* \to (\partial_{\mu}+i\epsilon_3A_{\mu})\varphi^*, \quad (3.2)$$

in the total Lagrangian for $\Sigma^{\pm} \to n+\pi^{\pm}$ systems, where the interaction Lagrangian (2.1) is assumed. In addition, the interaction between the electromagnetic field and anomalous moments for the hyperon and nucleon are included. We wish to evaluate the pion spectra to the square-term correction for the magnetic moments as the previously published calculation only included linear-term correction. Now, we would like to outline some procedures which will be helpful in under-

[7] L. Wolfenstein, Phys. Rev. **121**, 1245 (1961).

standing the more complicated pole model results to be discussed later. In the lowest order the Feynman diagrams responsible for these radiative decays are illustrated in Fig. 2. For $\Sigma^{\pm}\to n+\pi^{\pm}+\gamma$ decays we need only to consider the special case in which the nucleon charge $\epsilon_2=0$, and the hyperon charge is equal to the pion charge $\epsilon_1=\epsilon_2=e$. ϵ^{λ} is the photon polarization vector, where $\lambda=1, 2$ refers to the two transverse components. After some simplification, the decay amplitude A_{Ra} is

$$A_{\mathrm{Ra}}=\frac{1}{(2\pi)^2}\left(\frac{m_1}{E_1}\right)^{1/2}\left(\frac{m_2}{E_2}\right)^{1/2}\left(\frac{1}{2K}\right)^{1/2}\left(\frac{1}{2Q}\right)^{1/2}\frac{g}{\mu}$$
$$\times\tilde{W}^{s}(p_2)\Big\{ia\Big[+\boldsymbol{k}(\gamma\cdot\epsilon^{\lambda})\Big(\frac{-\mu_1(p_1\cdot k-m_1^2+m_1m_2)}{p_1\cdot k}+\frac{\mu_2(p_2\cdot k+m_2^2-m_1m_2)}{p_2\cdot k}+\frac{e(m_1-m_2)}{2p_1\cdot k}\Big)$$
$$+(\gamma\cdot\epsilon^{\lambda})(\mu_1+\mu_2)(m_1-m_2)-\mu_2\boldsymbol{k}(m_1-m_2)\frac{p_2\cdot\epsilon^{\lambda}}{p_2\cdot k}+e\frac{q\cdot\epsilon^{\lambda}}{q\cdot k}(m_1-m_2)\Big]$$
$$+b\gamma_5\Big[\boldsymbol{k}(\gamma\cdot\epsilon^{\lambda})\Big(\frac{-\mu_1(p_1\cdot k-m_1^2-m_1m_2)}{p_1\cdot k}-\frac{\mu_2(p_2\cdot k+m_2^2+m_1m_2)}{P_2\cdot k}+\frac{e(m_1+m_2)}{2p_1\cdot k}\Big)$$
$$+(\gamma\cdot\epsilon^{\lambda})(\mu_1-\mu_2)(m_1+m_2)+\mu_2\boldsymbol{k}(m_1+m_2)\frac{p_2\cdot\epsilon^{\lambda}}{p_2\cdot k}+e\frac{q\cdot\epsilon^{\lambda}}{q\cdot k}(m_1+m_2)\Big]\Big\}$$
$$\times W^{r}(p_1)\delta(p_1-p_2-q-k), \quad (3.3)$$

where $k=(\mathbf{k},K)$ is the four-momentum of the photon. From the above decay amplitude A_{Ra} it is possible to find the transition probability in the standard manner. The existence of the infrared divergence implies that the total transition probability is not well defined, and it leads to a logarithm divergence at the maximum pion energy, but we can sum up to a fixed pion energy. The differential transition probability for the radiative decay in the rest system of the hyperon is

$$\frac{dW_{\mathrm{Ra}}}{d|\mathbf{q}|}=\frac{|\mathbf{q}|}{2^4(2\pi)^3}\frac{1}{Qm_1}\left(\frac{g}{\mu}\right)^2\frac{2e^2}{m_1}\Big[(m_1\mp m_2)^2-\mu^2\Big]\Big[\frac{4m_1Q}{m_1^2+\mu^2-2m_1Q-m_2^2}\ln\Big(\frac{Q+|\mathbf{q}|}{Q-|\mathbf{q}|}\Big)-\frac{8m_1|\mathbf{q}|}{m_1^2+\mu^2-2m_1Q-m_2^2}$$
$$+\frac{m_1^2+\mu^2-2m_1Q-m_2^2}{(m_1\pm m_2)^2-\mu^2}\ln\Big(\frac{m_1-Q+|\mathbf{q}|}{m_1-Q-|\mathbf{q}|}\Big)\Big]+4e(m_1\mp m_2)(\mu_1\mp\mu_2)(m_1^2-m_2^2+\mu^2-2m_1Q)$$
$$\times\Big[\pm m_1m_2\frac{2|\mathbf{q}|}{m_1^2-2m_1Q+\mu^2}+\frac{\mu^2}{m_1}\ln\Big(\frac{Q+|\mathbf{q}|}{Q-|\mathbf{q}|}\Big)+\frac{1}{m_1}(\mu^2\mp m_1m_2)\ln\Big(\frac{m_1-Q+|\mathbf{q}|}{m_1-Q-|\mathbf{q}|}\Big)\Big]$$
$$+8\frac{m_1(m_1^2-m_2^2+\mu^2-2m_1Q)|\mathbf{q}|}{m_1^2-2m_1Q+\mu^2}\Big[(\mu_1\mp\mu_2)^2(m_1^2-m_2^2+\mu^2-2m_1Q)$$
$$\times\Big[\tfrac{1}{2}(-m_1-Q\pm2m_2)+\frac{m_2^2\pm2m_1m_2}{2(m_1^2-2m_1Q+\mu^2)}\Big]-(m_1\mp m_2)^2\frac{\mu_1\mu_2}{|\mathbf{q}|}\Big[\ln\Big(\frac{m_1-Q+|\mathbf{q}|}{m_1-Q-|\mathbf{q}|}\Big)$$
$$+2m_2\Big(\frac{m_2(m_1-Q)}{m_1^2-2m_1Q+\mu^2}\pm2\Big)\Big]\Big]+8(\mu_1\pm\mu_2)^2\frac{m_1(m_1\mp m_2)^2|\mathbf{q}|}{(m_1^2-2m_1Q+\mu^2)^2}(m_1^2-m_2^2+\mu^2-2m_1Q)^2$$
$$\times\Big[\frac{m_1^2-2m_1Q+\mu^2}{m_1^2-m_2^2+\mu^2-2m_1Q}(m_1-Q\pm m_2)-\tfrac{1}{2}(m_1-Q)\Big]+8\mu_1^2(m_1\mp m_2)^2(m_1^2-m_2^2+\mu^2-2m_1Q)$$
$$\times\Big[-\frac{m_1(m_1-Q)|\mathbf{q}|}{m_1^2-2m_1Q+\mu^2}+\frac{m_2}{2}\ln\Big(\frac{m_1-Q+|\mathbf{q}|}{m_1-Q-|\mathbf{q}|}\Big)\Big], \quad (3.4)$$

where the upper sign in $\pm$ or $\mp$ corresponds to $|a|=1$, $|b|=0$ (pure s-wave type); and the lower sign to $|a|=0$, $|b|=1$ (pure p-wave type). From Eqs. (2.3) and (3.4), we can calculate the branching ratio between the radiative and nonradiative decays either in the differential or integral form. In Figs. 3 and 4 (and

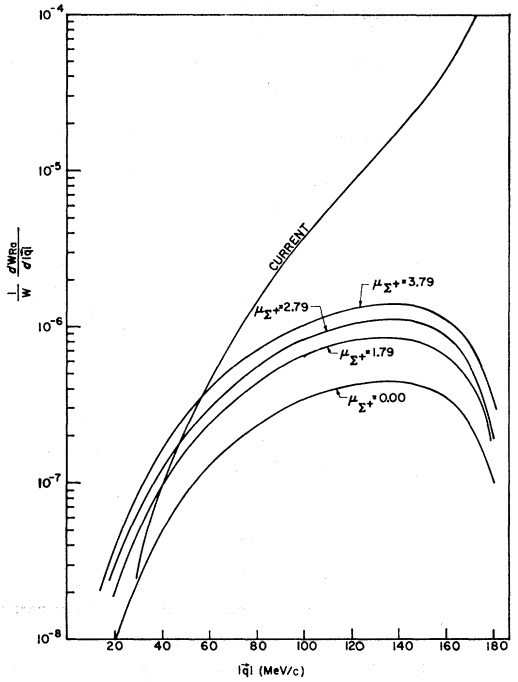

FIG. 3. Pion momentum spectrum of the differential values $W(\Sigma^+ \to n+\pi^+ +\gamma)/W(\Sigma^+ \to n+\pi^+)$ and its magnetic corrections for s wave $\Sigma^+ \to n+\pi^+$ as in Table I.

Tables I and II), we list the differential and integral π^+ spectra for Σ^+ radiative decay for s and p waves, respectively. The current contribution is from the Σ hyperon and π meson currents where all the magnetic moments are taken as zero. The magnetic moment contribution is the sum of the magnetic moment term as shown in Eq. (3.4). Note that the magnetic contributions are only significant for s waves and increase as μ_{Σ^+} increases, but are negligible for p waves. It is immediately apparent that the radiative decay branching ratios for the s-wave and p-wave decay hypotheses are quite different. This difference is much larger than the differences due to various assumptions about the Σ^+ magnetic moments. Tables III and IV contain the analogous results for Σ^- radiative decays. Both Σ^+ and Σ^- radiative decays have the same spectra except for a small pion energy shift. The shift comes from the mass difference of Σ^+ and Σ^- hyperons. Hence a measurement for Σ^+ and Σ^- radiative decays can be used to determine the s- or p-wave nature of each of these nonradiative decays.

We should point out that the magnetic corrections calculated here are different and somewhat greater than those of Nauenberg *et al.*[1] They calculated only the linear correction term. In our case the square term was also included. The calculations show that both the linear and quadratic terms are of the same order, and that in some cases the square term may be greater. This result contradicts the conventional treatment of a small correction in the γ-matrix calculations. As one handles a small correction proportional to a γ matrix, the square term is not always smaller than the linear correction. A concrete example is

$$1+\alpha\gamma_5.$$

The trace of this matrix square gives

$$\tfrac{1}{4}\mathrm{Tr}[(1+\alpha\gamma_5)(1+\alpha^*\gamma_5)]=1+\alpha^2.$$

This peculiar property is directly related to the different behavior of traces of even and odd products of γ matrices. In fact the single current term of fermion involves odd γ matrices and the single magnetic term involves even γ matrices.

The Σ^- hyperon is slightly heavier than the Σ^+ hyperon. For a fixed pion momentum the γ ray from Σ^- hyperons is more energetic than that from Σ^+ hyperons. If the pion momentum is 160 MeV/c, the total transition probability from the current contributions are

$$\begin{aligned} \Sigma^+ \quad & s \text{ wave} \quad 0.99 \times 10^{-3}, \\ & p \text{ wave} \quad 0.123 \times 10^{-2}, \\ \Sigma^- \quad & s \text{ wave} \quad 0.79 \times 10^{-3}, \\ & p \text{ wave} \quad 0.104 \times 10^{-2}. \end{aligned}$$

It suggests that one can even use the higher pion momentum spectra to distinguish s or p waves provided the pion momentum could be measured accurately.

IV. POLE-MODEL CALCULATIONS

The preceding section was based on the phenomenological interactions given in Eqs. (2.1) and (3.1). But

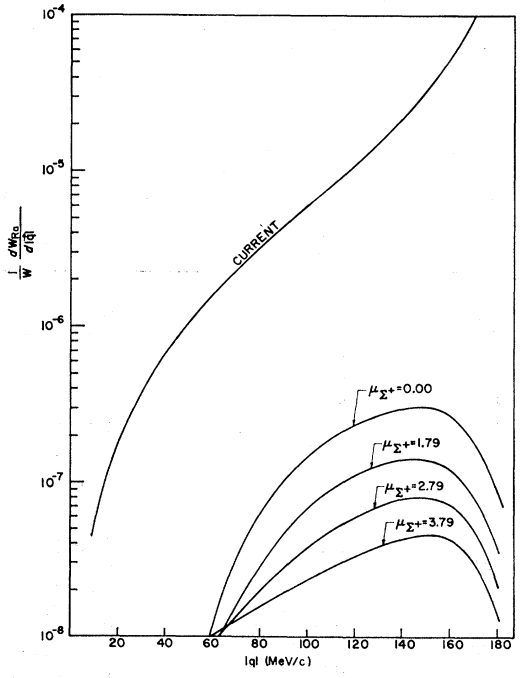

FIG. 4. Pion momentum spectrum of the differential value $W(\Sigma^+ \to n+\pi^+ +\gamma)/W(\Sigma^+ \to n+\pi^+)$ and its magnetic corrections for p wave $\Sigma^+ \to n+\pi^+$ as in Table II.

TABLE I. The differential and integral value of $w(\Sigma^+ \to n+\pi^++\gamma)/w(\Sigma^+ \to n+\pi^+)$ as a function of pion momentum, q, for s wave $\Sigma^+ \to n+\pi^+$ decay. (The definition of "current" and "magnetic moment" contributions are contained in the text.)

$\|q\|$	Current contribution	Magnetic moment corrections $\mu_{\Sigma^+}=3.79$	$\mu_{\Sigma^+}=2.79$	$\mu_{\Sigma^+}=1.79$	$\mu_{\Sigma^+}=0.00$
		Differential			
20	0.69×10^{-8}	0.29×10^{-7}	0.22×10^{-7}	0.157×10^{-7}	0.69×10^{-8}
40	0.91×10^{-7}	0.133×10^{-6}	0.85×10^{-7}	0.61×10^{-7}	0.26×10^{-7}
60	0.44×10^{-6}	0.24×10^{-6}	0.184×10^{-6}	0.131×10^{-6}	0.57×10^{-7}
80	0.138×10^{-5}	0.41×10^{-6}	0.31×10^{-6}	0.216×10^{-6}	0.93×10^{-7}
100	0.35×10^{-5}	0.58×10^{-6}	0.43×10^{-6}	0.30×10^{-6}	0.128×10^{-6}
120	0.80×10^{-5}	0.72×10^{-6}	0.53×10^{-6}	0.37×10^{-6}	0.155×10^{-6}
140	0.180×10^{-4}	0.77×10^{-6}	0.57×10^{-6}	0.39×10^{-6}	0.161×10^{-6}
160	0.46×10^{-4}	0.64×10^{-6}	0147×10^{-6}	0.32×10^{-6}	0.129×10^{-6}
180	0.31×10^{-3}	0.187×10^{-6}	0.137×10^{-6}	0.94×10^{-7}	0.37×10^{-7}
		Integral			
20	0.29×10^{-7}	0.179×10^{-6}	0.135×10^{-6}	0.97×10^{-7}	0.43×10^{-7}
40	0.72×10^{-6}	0.147×10^{-5}	0.111×10^{-5}	0.79×10^{-6}	0.35×10^{-6}
60	0.51×10^{-5}	0.49×10^{-5}	0.37×10^{-5}	0.26×10^{-5}	$0\ 116 \times 10^{-5}$
80	$0\ 21 \times 10^{-4}$	$0\ 11 \times 10^{-4}$	0.85×10^{-5}	0.60×10^{-5}	0.26×10^{-5}
100	0.67×10^{-4}	0.21×10^{-4}	0.158×10^{-4}	0.112×10^{-4}	0.48×10^{-5}
120	0.174×10^{-3}	0.34×10^{-4}	0.25×10^{-4}	0.180×10^{-4}	0.77×10^{-5}
140	0.41×10^{-3}	0.49×10^{-4}	0.36×10^{-4}	0.258×10^{-4}	0.109×10^{-4}
160	0.99×10^{-3}	0.64×10^{-4}	0.47×10^{-4}	0.33×10^{-4}	0.139×10^{-4}
180	0.32×10^{-2}	0.73×10^{-4}	0.54×10^{-4}	0.38×10^{-4}	0.157×10^{-4}

there still remain some questions, namely, whether the results are model dependent, and if so to what extent. We wish to examine the problem further. To describe the nonradiative hyperon decay, the model does not matter, since a change leads only to a coupling constant readjustment. But for the radiative hyperon decays the situation is different, since some momenta will be off the mass shell. The form factors for the hyperon weak vertices will enter the problem; these can influence the radiative decay rate. So the details of the vertex for hyperon decay have to be studied. This is done by using a structure based on the pole approach. Originally, the pole approximation comes from the pole term on the dispersion relation. It can give a correlation between the coupling constants in the strong interaction and in the weak interaction. This problem has been studied by various authors for the nonleptonic hyperon decay.[6] The interactions which are considered as fundamental are the usual three-point functions for the strong interaction and the two-point weak interactions where the two interacting particles have their strangeness differing by one unit. This last interaction includes a parity conserving part and a parity nonconserving part. In the discussion that follows, the influence of some individual

TABLE II. The differential and integral values of $w(\Sigma^+ \to n+\pi^++\gamma)/w(\Sigma^+ \to n+\pi^+)$ as a function of pion momentum, q, for p wave $\Sigma^+ \to n+\pi^+$ decay.

$\|q\|$	Current contribution	Magnetic moment corrections $\mu_{\Sigma^+}=3.79$	$\mu_{\Sigma^+}=2.79$	$\mu_{\Sigma^+}=1.79$	$\mu_{\Sigma^+}=0.00$
		Differential			
20	0.177×10^{-6}	0.159×10^{-8}	0.51×10^{-9}	-0.53×10^{-9}	-0.23×10^{-8}
40	0.72×10^{-6}	0.56×10^{-8}	0.27×10^{-8}	0.37×10^{-9}	-0.27×10^{-8}
60	0.170×10^{-5}	0.107×10^{-7}	0.85×10^{-8}	0.85×10^{-8}	$+0.139 \times 10^{-7}$
80	0.33×10^{-5}	0.163×10^{-7}	0.199×10^{-7}	0.29×10^{-7}	0.61×10^{-7}
100	0.59×10^{-5}	0.233×10^{-7}	0.37×10^{-7}	0.63×10^{-7}	0.139×10^{-6}
120	0.106×10^{-4}	0.32×10^{-7}	0.58×10^{-7}	0.103×10^{-6}	0.23×10^{-6}
140	0.204×10^{-4}	0.42×10^{-7}	0.76×10^{-7}	0.134×10^{-6}	0.29×10^{-6}
160	0.48×10^{-4}	0.43×10^{-7}	0.73×10^{-7}	0.127×10^{-6}	0.28×10^{-6}
180	0.31×10^{-3}	0.156×10^{-7}	0.24×10^{-7}	0.411×10^{-7}	0.90×10^{-7}
		Integral			
20	0.110×10^{-5}	0.100×10^{-7}	0.30×10^{-8}	-0.39×10^{-8}	-0.159×10^{-7}
40	0.92×10^{-5}	0.77×10^{-7}	0.39×10^{-7}	-0.127×10^{-7}	-0.80×10^{-7}
60	0.32×10^{-4}	0.23×10^{-6}	0.133×10^{-6}	0.55×10^{-7}	-0.183×10^{-7}
80	0.80×10^{-4}	0.50×10^{-6}	0.40×10^{-6}	0.40×10^{-6}	0.65×10^{-6}
100	0.168×10^{-3}	0.89×10^{-6}	0.95×10^{-6}	0.129×10^{-5}	0.24×10^{-5}
120	0.32×10^{-3}	0.144×10^{-5}	0.190×10^{-5}	0.29×10^{-5}	0.62×10^{-5}
140	0.61×10^{-3}	0.22×10^{-5}	0.32×10^{-5}	0.53×10^{-5}	0.115×10^{-4}
160	0.123×10^{-2}	0.31×10^{-5}	0.48×10^{-5}	0.80×10^{-5}	0.176×10^{-4}
180	0.34×10^{-2}	0.37×10^{-5}	0.59×10^{-5}	0.99×10^{-5}	0.218×10^{-4}

TABLE III. The differential and integral values of $w(\Sigma^- \to n+\pi^-+\gamma)/w(\Sigma^- \to n+\pi^-)$ as a function of pion momentum q for s wave $\Sigma^- \to n+\pi^-$ decay.

$\|q\|$	Current contribution	Magnetic moment corrections $\mu_{\Sigma^-}=1.00$	$\mu_{\Sigma^-}=0.00$	$\mu_{\Sigma^-}=-0.83$	$\mu_{\Sigma^-}=-1.83$
		Differential			
20	0.64×10^{-8}	0.111×10^{-7}	0.68×10^{-8}	0.39×10^{-8}	0.121×10^{-8}
40	0.81×10^{-7}	0.43×10^{-7}	0.26×10^{-7}	0.150×10^{-7}	0.46×10^{-8}
60	0.39×10^{-6}	0.93×10^{-7}	0.56×10^{-7}	0.32×10^{-7}	0.96×10^{-8}
80	0.122×10^{-5}	0.154×10^{-6}	0.92×10^{-7}	0.51×10^{-7}	0.154×10^{-7}
100	0.30×10^{-5}	0.21×10^{-6}	0.129×10^{-6}	0.69×10^{-7}	0.21×10^{-7}
120	0.67×10^{-5}	0.27×10^{-6}	0.160×10^{-6}	0.87×10^{-7}	0.25×10^{-7}
140	0.145×10^{-4}	0.30×10^{-6}	0.174×10^{-6}	0.93×10^{-7}	0.26×10^{-7}
160	0.34×10^{-4}	0.27×10^{-6}	0.156×10^{-6}	0.83×10^{-7}	0.23×10^{-7}
180	0.116×10^{-3}	0.153×10^{-6}	0.87×10^{-7}	0.45×10^{-7}	0.122×10^{-7}
		Integral			
20	0.271×10^{-7}	0.69×10^{-7}	0.42×10^{-7}	0.24×10^{-7}	0.75×10^{-8}
40	0.65×10^{-6}	0.57×10^{-6}	0.34×10^{-6}	0.197×10^{-6}	0.61×10^{-7}
60	0.46×10^{-5}	0.188×10^{-5}	0.114×10^{-5}	0.65×10^{-6}	0.199×10^{-6}
80	0.191×10^{-4}	0.43×10^{-5}	0.261×10^{-5}	0.147×10^{-5}	0.44×10^{-6}
100	0.58×10^{-4}	0.80×10^{-5}	0.48×10^{-5}	0.27×10^{-5}	0.80×10^{-6}
120	0.150×10^{-3}	0.129×10^{-4}	0.77×10^{-5}	0.43×10^{-5}	0.127×10^{-5}
140	0.35×10^{-3}	0.187×10^{-4}	0.110×10^{-4}	0.61×10^{-5}	0.178×10^{-5}
160	0.79×10^{-3}	0.25×10^{-4}	0.144×10^{-4}	0.79×10^{-5}	0.23×10^{-5}
180	0.200×10^{-2}	0.29×10^{-4}	0.170×10^{-4}	0.93×10^{-5}	0.26×10^{-5}

pole structure on the radiative decay is given. The requirements for isospin nonvariance on the strong interactions and $\Delta I=\frac{1}{2}$ rule on the weak interaction are not imposed, since we are only interested in estimating the importance of some decay structures on the theoretical radiative decay rate.

A. Proton Pole

If the nonleptonic Σ^+ decay is dominated by the proton pole, the decay process corresponds to the diagram of Fig. 5. In this figure, the circle represents the strong vertex which has the form

$$g_1\tilde{W}^s(p_2)\boldsymbol{q}\gamma_5 W^t(p). \tag{4.1}$$

FIG. 5. Feynman diagram for $\Sigma^+ \to n+\pi^+$ decay in the proton pole model.

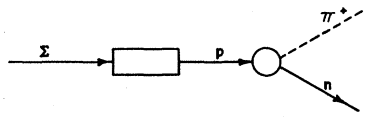

The weak two-point vertex, represented by the rectangular box, is chosen as

$$\tilde{W}^t(p)(a_1\gamma_5+ib_1)W^r(p_1), \tag{4.2}$$

TABLE IV. The differential and integral values of $w(\Sigma^- \to n+\pi^-+\gamma)/(w(\Sigma^- \to n+\pi^-)$ as a function of pion momentum q for p wave $\Sigma^- \to n+\pi^-$ decay.

$\|q\|$	Current contribution	Magnetic moment corrections $\mu_{\Sigma^-}=1.00$	$\mu_{\Sigma^-}=0.00$	$\mu_{\Sigma^-}=-0.83$	$\mu_{\Sigma^-}=-1.83$
		Differential			
20	0.166×10^{-6}	-0.137×10^{-8}	-0.24×10^{-8}	-0.32×10^{-8}	-0.41×10^{-8}
40	0.68×10^{-6}	-0.154×10^{-8}	-0.33×10^{-8}	-0.43×10^{-8}	-0.52×10^{-8}
60	0.159×10^{-5}	0.87×10^{-8}	-0.117×10^{-7}	0.157×10^{-7}	0.23×10^{-7}
80	0.30×10^{-5}	0.38×10^{-7}	0.56×10^{-7}	0.75×10^{-7}	0.103×10^{-6}
100	0.54×10^{-5}	0.87×10^{-7}	0.131×10^{-6}	0.176×10^{-6}	0.24×10^{-6}
120	0.93×10^{-5}	0.149×10^{-6}	0.23×10^{-6}	0.30×10^{-6}	0.41×10^{-6}
140	0.170×10^{-4}	0.203×10^{-6}	0.31×10^{-6}	0.41×10^{-6}	0.56×10^{-6}
160	0.35×10^{-4}	0.21×10^{-6}	0.33×10^{-6}	0.43×10^{-6}	0.59×10^{-6}
180	0.117×10^{-3}	0.134×10^{-6}	0.210×10^{-6}	0.27×10^{-6}	0.37×10^{-6}
		Integral			
20	0.103×10^{-5}	-0.94×10^{-8}	-0.160×10^{-7}	-0.215×10^{-7}	-0.28×10^{-7}
40	0.86×10^{-5}	-0.47×10^{-7}	-0.85×10^{-7}	-0.114×10^{-6}	-0.145×10^{-6}
60	0.30×10^{-4}	-0.65×10^{-8}	-0.47×10^{-7}	-0.62×10^{-7}	-0.57×10^{-7}
80	0.75×10^{-4}	0.41×10^{-6}	0.55×10^{-6}	0.74×10^{-6}	0.106×10^{-5}
100	0.155×10^{-3}	0.161×10^{-5}	0.23×10^{-5}	0.31×10^{-5}	0.43×10^{-5}
120	0.30×10^{-3}	0.39×10^{-5}	0.58×10^{-5}	0.78×10^{-5}	0.108×10^{-4}
140	0.55×10^{-3}	0.75×10^{-5}	0.112×10^{-4}	0.150×10^{-4}	0.205×10^{-4}
160	0.104×10^{-2}	0.118×10^{-4}	0.176×10^{-4}	0.24×10^{-4}	0.32×10^{-4}
180	0.32×10^{-2}	0.154×10^{-4}	0.23×10^{-4}	0.31×10^{-4}	0.43×10^{-4}

where g_1, a_1, and b_1 are the coupling constants. $W^t(p)$ is the spinor of the proton. The decay amplitude can be written directly as Eq. (2.2)

$$A_1 \equiv ig_1(2\pi)^{-1/2}\delta(p_1-q-p_2)\left(\frac{m_1m_2}{E_1E_2 2Q}\right)^{1/2}\bar{W}^s(p_2)$$
$$\times\left(-a_1\frac{1}{m_1+m_2}+ib_1\gamma_5\frac{1}{m_1-m_2}\right)\boldsymbol{q}W^r(p_1). \quad (4.3)$$

The differences between the amplitude A (2.2) and A_1 (4.3) are only the replacements of the coupling constants, as follows:

$$a(g/\mu)=a_1g_1[1/(m_1+m_2)];$$
$$b(g/\mu)=b_1g_1[1/(m_1-m_2)]. \quad (4.4)$$

Hence we do not have to go through all the calculations. All the necessary results can be written down from II with the appropriately changed coupling constants. The subscript 1 is introduced to denote the corresponding formula. For example, the decay transition probability per unit time for this model is

$$W_1 \equiv g_1^2\frac{1}{8\pi m_1^2}\left[\left(\frac{m_1^2-m_2^2+\mu^2}{2m_1}\right)^2-\mu^2\right]^{1/2}$$
$$\times\left\{\left(\frac{a_1}{m_1+m_2}\right)^2(m_1-m_2)^2[(m_1+m_2)^2-\mu^2]\right.$$
$$\left.+\left(\frac{b_1}{m_1-m_2}\right)(m_1+m_2)^2[(m_1-m_2)^2-\mu^2]\right\} \quad (4.5)$$

which is the same as (2.3) except for some constants. The electromagnetic interaction for the diagram Fig. 5 can be introduced in the same way as was done for the diagram Fig. 1. The diagrams for the corresponding Σ^+ radiative decays are illustrated in Fig. 6. The corresponding decay amplitude, $A_{1\mathrm{Ra}}$, obtained after some simplifications, is

$$A_{1\mathrm{Ra}} \equiv -ig_1\frac{1}{(2\pi)^2}\left(\frac{m_1}{E_1}\right)^{1/2}\left(\frac{m_2}{E_2}\right)^{1/2}\left(\frac{1}{2K}\right)^{1/2}\left(\frac{1}{Q2}\right)^{1/2}\bar{W}^s(p_2)\left\{\boldsymbol{q}\gamma_5\frac{1}{(\boldsymbol{p}_2+\boldsymbol{q})-m_2}(a_1\gamma_5+ib_1)\frac{1}{(\boldsymbol{p}_2+\boldsymbol{q})-m_1}\right.$$
$$[-\epsilon_1(\gamma\cdot\epsilon^\lambda)+\mu_1\boldsymbol{k}(\gamma\cdot\epsilon^\lambda)]+\boldsymbol{q}\gamma_5\frac{1}{(\boldsymbol{p}_2+\boldsymbol{q})-m_2}(-\epsilon_p+\mu_p\boldsymbol{k})(\gamma\cdot\epsilon^\lambda)\frac{1}{\boldsymbol{p}_1-m_2}(a_1\gamma_5+ib_1)$$
$$+\epsilon_3(\gamma\cdot\epsilon^\lambda)\gamma_5\frac{1}{\boldsymbol{p}_1-m_2}(a_1\gamma_5+ib_1)-(\boldsymbol{q}+\boldsymbol{k})\gamma_5\frac{1}{\boldsymbol{p}_1-m_2}(a_1\gamma_5+ib_1)\frac{\epsilon_3(2q+k)\cdot\epsilon^\lambda}{(q+k)^2-\mu^2}$$
$$\left.+[-\epsilon_2(\gamma\cdot\epsilon^\lambda)+\mu_2\boldsymbol{k}(\gamma\cdot\epsilon^\lambda)]\frac{1}{\boldsymbol{p}_2+\boldsymbol{k}-m_2}\boldsymbol{q}\gamma_5\frac{1}{\boldsymbol{p}_1-m_2}(a_1\gamma_5+ib_1)\right\}W^r(p_1)\delta(p_1-p_2-q-k), \quad (4.6)$$

where ϵ_p and μ_p are the charge and magnetic moment of the proton, respectively. The amplitude $A_{1\mathrm{Ra}}$ in the form of Eq. (4.6) can be reduced to the following by using the properties of the γ matrices.

$$A_{1\mathrm{Ra}}=\frac{1}{(2\pi)^2}\left(\frac{m_1}{E_1}\right)^{1/2}\left(\frac{m_2}{E_2}\right)^{1/2}\left(\frac{1}{2K}\right)^{1/2}\left(\frac{1}{2Q}\right)^{1/2}g_1\bar{W}^s(p_2)\left[\frac{a_1i}{m_1+m_2}\left[\boldsymbol{k}(\gamma\cdot\epsilon^\lambda)\right.\right.$$
$$\times\left\{\frac{-\mu_1(p_1\cdot k-m_1^2+m_1m_2)}{p_1\cdot k}+\frac{\mu_2(p_2\cdot k+m_2^2-m_1m_2)}{p_2\cdot k}+\frac{e(m_1-m_2)}{2p_1\cdot k}+\frac{\mu_1+\mu_p}{(p_2+q)^2-m_2^2}[(m_1-m_2)^2-2p_1\cdot k]\right\}$$
$$+(\gamma\cdot\epsilon^\lambda)\left((\mu_1+\mu_2)(m_1-m_2)-(\mu_1+\mu_p)\frac{4m_2p_1\cdot k}{(p_2+q)^2-m_2^2}\right)-\mu_2\boldsymbol{k}(m_1-m_2)\frac{p_2\cdot\epsilon^\lambda}{p_2\cdot k}+e\frac{q\cdot\epsilon^\lambda}{q\cdot k}(m_1-m_2)\Big]$$
$$+\frac{b_1}{m_1-m_2}\left(\boldsymbol{k}(\gamma\cdot\epsilon^\lambda)\left\{\frac{-\mu_1(p_1\cdot k-m_1^2-m_1m_2)}{p_1\cdot k}-\frac{\mu_2(p_2\cdot k+m_2^2+m_1m_2)}{p_2\cdot k}+\frac{e(m_1+m_2)}{2p_1\cdot k}\right.\right.$$
$$\left.+\frac{\mu_1+\mu_p}{(p_2+q)^2-m_2^2}[(m_1+m_2)^2-2p_1\cdot k]\right\}+(\gamma\cdot\epsilon^\lambda)\left[(\mu_1-\mu_2)(m_1+m_2)+(\mu_1+\mu_p)\frac{4m_2p_1\cdot k}{(p_2+q)^2-m_2^2}\right]$$
$$\left.\left.+\mu_2\boldsymbol{k}(m_1+m_2)\frac{p_2\cdot\epsilon^\lambda}{p_2\cdot k}+e\frac{q\cdot\epsilon^\lambda}{q\cdot k}(m_1-m_2)\right)\right]W^r(p_1)\delta(p_1-p_2-q-k). \quad (4.7)$$

The difference between Eq. (3.3) and Eq. (4.7) occurs only in the terms containing the anomalous magnetic moments. Hence we expect that in the proton pole approximation the essential features of the radiative decay remain unchanged. The evaluation of the corresponding differential transition probability is laborious but straightforward. It is possible to express the differential transition probability in terms of known functions. Since we are interested only in numerical values, it is wise to use the computer directly to evaluate the integrals, instead of writing lengthy differential transition probability expressions. The results of the numerical calculation will be presented and discussed in Sec. V.

B. Neutral (Λ or Σ^0) Poles

In the same manner as shown immediately above we can consider the $\Sigma^{\pm}$ decays being dominated by the neutral hyperon poles. Both neutral poles will give the same decay structures which are different from that of the charged proton pole. Hence the discussion of each can be combined. The decay process corresponds to the diagram shown in Fig. 7. In Fig. 7 the circle represents the strong vertex which has the form

$$g_2\tilde{W}^t(p)\boldsymbol{q}\gamma_5 W^r(p_1).$$

The weak two-point vertex, represented by the rectangular box, is chosen as

$$\tilde{W}^s(p_2)(a_2\gamma_5+ib_2)W^t(p), \tag{4.8}$$

where g_2, a_2, and b_2 are the coupling constants. $W^t(p)$ is the spinor of the intermediate neutral hyperon. The corresponding decay transition probability per unit time for this model is

$$W_2\equiv g_2^2\frac{1}{8\pi m_1^2}\left[\left(\frac{m_1^2-m_2^2+\mu^2}{2m_1}\right)^2-\mu^2\right]^{1/2}$$
$$\times\left\{\left(\frac{a_2}{m_2+m}\right)^2(m_1-m_2)[(m_1+m_2)^2-\mu^2]+\left(\frac{b_2}{m_2-m}\right)^2(m_1+m_2)^2[(m_1-m_2)^2-\mu^2]\right\}, \tag{4.9}$$

where m is the mass of the neutral hyperon. The electromagnetic interaction can be introduced in the same way as in the case of charged proton. The $\Sigma^{\pm}$ radiative decay diagrams are shown in Fig. 8. The decay amplitude for these diagrams has the form

$$A_{2\mathrm{Ra}}\equiv\frac{1}{(2\pi)^2}\left(\frac{m_1}{E_1}\right)^{1/2}\left(\frac{m_2}{E_2}\right)^{1/2}\left(\frac{1}{2K}\right)^{1/2}\left(\frac{1}{2Q}\right)^{1/2}(-g_2)\tilde{W}^s(p_2)\frac{ia_2}{m+m_2}$$
$$\times\left\{\boldsymbol{k}(\gamma\cdot\epsilon^\lambda)\left[\frac{-\mu_1(p_1\cdot k-m_1^2+m_1m_2)}{p_1\cdot k}+\frac{\mu_2(p_2\cdot k+m_2^2-m_1m_2)}{p_2\cdot k}+\frac{e(m_1-m_2)}{2p_1\cdot k}\right.\right.$$
$$\left.+\frac{\mu_0+\mu_2}{(p_1-q)^2-m^2}(2p_1\cdot q-q^2-2m_1m+2mm_2)\right]+(\gamma\cdot\epsilon^\lambda)\left[(\mu_1+\mu_2)(m_1-m_2)-(\mu_0+\mu_2)\frac{4m_2p_2\cdot k}{(p_1-q)^2-m^2}\right]$$
$$\left.+\boldsymbol{k}\left[-\mu_2\frac{p_2\cdot\epsilon^\lambda}{p_2\cdot k}(m_1-m_2)+(\mu_0+\mu_2)\frac{4m_2p_2\cdot\epsilon^\lambda}{(p_1-q)^2-m^2}\right]+e\frac{q\cdot\epsilon^\lambda}{q\cdot k}(m_1-m_2)\right\}$$
$$+\frac{b_2}{m-m_2}\left\{\boldsymbol{k}(\gamma\cdot\epsilon^\lambda)\left[\frac{-\mu_1(p_1\cdot k-m_1^2-m_1m_2)}{p_1\cdot k}-\frac{\mu_2(p_2\cdot k+m_2^2+m_1m_2)}{p_2\cdot k}+\frac{e(m_1+m_2)}{2p_1\cdot k}+\frac{\mu_0-\mu_2}{(p_1-q)^2-m^2}\right.\right.$$
$$\left.\times(2p_1\cdot q-q^2-2m_1m-2mm_2)\right]+(\gamma\cdot\epsilon^\lambda)\left[(\mu_1-\mu_2)(m_1+m_2)+(\mu_0-\mu_2)\frac{4m_2p_2\cdot k}{(p_1-q)^2-m^2}\right]$$
$$\left.+\left[\boldsymbol{k}\mu_2\frac{p_2\cdot\epsilon^\lambda}{p_2\cdot k}(m_1+m_2)-(\mu_0-\mu_2)\frac{4m_2p_2\cdot\epsilon^\lambda}{(p_1-q)^2-m^2}\right]+e\frac{q\cdot\epsilon^\lambda}{q\cdot k}(m_1+m_2)\right\}W^r(p_1)\delta(p_1-p_2-q-k), \tag{4.10}$$

where μ_0 is the magnetic moment of the neutral hyperon. If we compare with the first model described in Sec. III, and particularly with Eq. (3.3), we observe the same fact as in the proton pole case that the neutral pole model still yields a correction of the order of the anomalous magnetic moments. In general, if one

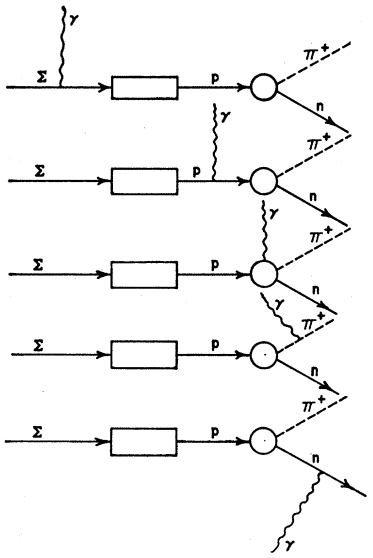

FIG. 6. Feynman diagrams for $\Sigma^+ \to n+\pi^+ +\gamma$ decay in the proton pole model.

assumes that the $\Sigma^\pm \to n+\pi^\pm$ decays are dominated by other poles, such as a K pole, then the discrepancy with the model in Sec. III is only of the order of the anomalous magnetic moments. As we shall see, the current contribution is always the dominant term in the radiative hyperon decays, so we will not discuss any other pole models in detail.

C. Virtual K-Meson Loops

The decay vertex structures just discussed were based on the pole approach. In this model the intermediate particles in the reaction have low velocities, and consequently their contributions to inner bremsstrahlung may dominate the radiative nonleptonic decay, so we would like to examine the loop contributions. In the

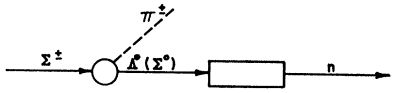

FIG. 7. Feynman diagrams for $\Sigma^\pm \to n+\pi^\pm$ decays in the Λ or Σ^0 pole model.

language of dispersion relations, the loop diagrams are related to contributions from the cuts in the complex plane, as distinguished from the pole contributions. The lowest intermediate mass cut or loop involves virtual K mesons, as in the diagram shown in Fig. 9. The circle represents strong interaction vertices, and the weak vertex is represented by the rectangular box. This kind of diagram gives rise to a parity nonconserving s-wave decay amplitude. For simplicity we choose the vertices as follows. All the strong interactions take the pseudoscalar forms

$$G_1\bar{W}^t(p)\gamma_5 W^r(p_1) \quad \text{for } \Sigma^\pm(\pi^\pm\Sigma^0) \text{ vertex, or for } \Sigma^\pm(\pi^\pm\Lambda) \text{ vertex,}$$

$$G_2\bar{W}^s(p_2)\gamma_5 W^t(p) \quad \text{for } \Sigma^0(\bar{K}^0 N) \text{ vertex, or for } \Sigma^\pm(\pi^\pm\Lambda) \text{ vertex,}$$

and the weak interaction is assumed to be a scalar given by

$$B \qquad \text{for } (\pi^\pm\bar{K}^0)\pi^\pm \text{ vertex,}$$

where G_1, G_2, and B are the corresponding coupling constants. In the conventional way the decay Feynman amplitude can be written down as

$$A_{3S}\equiv G_1G_2B(2\pi)^{-9/2}\left(\frac{m_1}{E_1}\right)^{1/2}\left(\frac{m_2}{E_2}\right)^{1/2}\left(\frac{1}{2Q}\right)^{1/2}$$
$$\times\delta(p_1-p_2-q)\int d^4p\,\bar{W}^s(p_2)\frac{\not{p}-m}{p^2-m^2}$$
$$\times\frac{1}{(p_1-p)^2-\mu^2}\frac{1}{(p-p_2)^2-\mu_K{}^2}W^r(p_1), \quad (4.11)$$

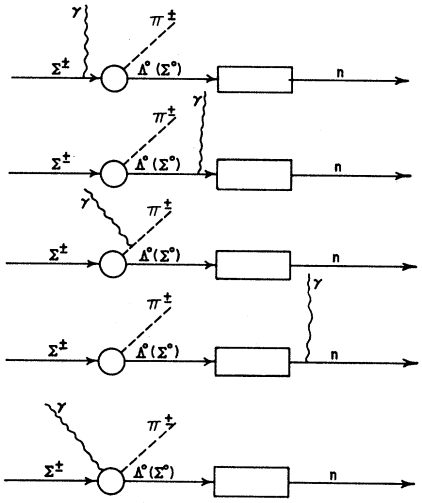

FIG. 8. Feynman diagrams for $\Sigma^\pm \to n+\pi^\pm+\gamma$ decays in the Λ or Σ^0 pole model.

where μ_K is the mass of the $\bar{K}^0$ meson. The integration above is not divergent and can be carried out by using the Feynman integration

$$\frac{1}{abc}=2\int_0^1 dx\int_0^x dy\frac{1}{[(a-b)y+(b-c)x+c]^3}, \quad (4.12)$$

and

$$\int d^4k(k^2-2p\cdot k-c)^{-3}=\frac{\pi}{2i}(p^2+c)^{-1},$$
$$\int d^4k\,k_\mu(k^2-2p\cdot k-c)^{-3}=\frac{\pi^2}{2i}p_\mu(p^2+c)^{-1}. \quad (4.13)$$

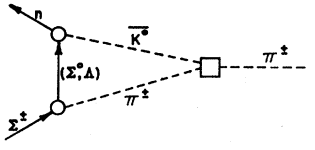

FIG. 9. Feynman diagram for $\Sigma^\pm \to n+\pi^\pm$ decays in the virtual K-meson loops.

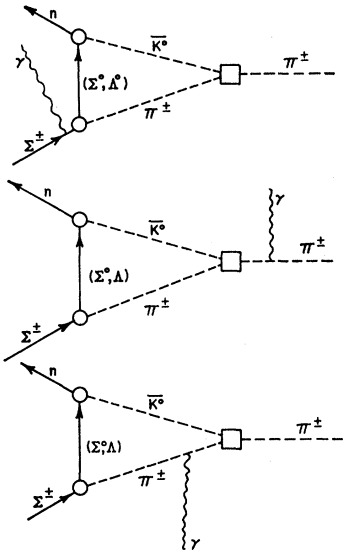

FIG. 10. Feynman diagrams for $\Sigma^{\pm}\to n+\pi^{\pm}+\gamma$ decays in the virtual K-meson loops.

Then the decay Feynman amplitude (4.11) reduces to

$$A_{3S}=G_1G_2B(2\pi)^{-9/2}\left(\frac{m_1}{E_1}\right)^{1/2}\left(\frac{m_2}{E_2}\right)^{1/2}\left(\frac{1}{2Q}\right)^{1/2}\times\delta(p_1-p_2-q)\tilde{W}^s(p_2)W^r(p_1)X, \quad (4.14)$$

where

$$X=-i\pi^2\int_0^1 dx\int_0^x dy\frac{Dy+E}{Cy^2+By+A} \quad (4.15)$$

and

$$A=m_2^2x^2-(m_2^2-\mu^2+m^2)x+m^2,$$
$$B=2xp_1\cdot p_2-2xm_2^2-(m_1^2-\mu^2-m_2^2+\mu_K^2),$$
$$C=\mu^2,\quad D=m_1-m_2,\quad E=m_2x-m. \quad (4.16)$$

The corresponding decay transition probability in the rest frame of the hyperon is

$$W_{3S}\equiv|G_1G_2B|^2\frac{1}{4(2\pi)^9}\frac{1}{m_1^2}[(m_1+m_2)^2-\mu^2]\times\left[\left(\frac{m_1^2+\mu^2-m_2^2}{2m_1}\right)^2-\mu^2\right]^{1/2}|X|^2. \quad (4.17)$$

Now we would like to introduce the electromagnetic interaction into the decay model. Since we chose baryon vertices as scalars, the radiative corrections coming from these baryon vertices are zero. In order to simplify the computation, the magnetic moment contribution from the baryons is completely ignored. Then the radiative decay diagrams are as shown in Fig. 10. The corresponding decay amplitude $A_{3\mathrm{Ra}S}$ is

$$A_{3\mathrm{Ra}S}\equiv-(2\pi)^{-6}G_1G_2B\left(\frac{m_1}{E_1}\right)^{1/2}\left(\frac{m_2}{E_2}\right)^{1/2}\left(\frac{1}{2K}\right)^{1/2}\left(\frac{1}{2Q}\right)^{1/2}e\delta(p_1-p_2-q-k)$$
$$\times\tilde{W}^s(p_2)\int\left[\frac{\not p-m}{p^2-m^2}\frac{2(p_1-k)\cdot\epsilon^\lambda+(\gamma\cdot\epsilon^\lambda)\not k}{-2p_1\cdot k}\frac{1}{(p-p_2)^2-\mu_K^2}\frac{1}{(p_1-k-p)^2-\mu^2}\right.$$
$$+\frac{\not p-m}{p^2-m^2}\frac{1}{(p-p_2)^2-\mu_K^2}\frac{1}{(p-p_1)^2-\mu^2}\frac{2q\cdot\epsilon^\lambda}{(q+k)^2-\mu^2}+\frac{\not p-m}{p^2-m^2}\frac{1}{(p-p_2)^2-\mu_K^2}$$
$$\left.\times\frac{1}{(p-p_1)^2-\mu^2}\frac{2(p_1-p)\cdot\epsilon^\lambda}{(p_1-p-k)^2-\mu^2}\right]W^r(p_1)d^4p. \quad (4.18)$$

The reduction of the decay amplitude $A_{3\mathrm{Ra}S}$ is carried out by using the Feynman integrations (4.12) and

$$\frac{1}{abcd}=6\int_0^1 dx\int_0^x dy\int_0^y dz\{(a-b)z+(b-c)y+(c-d)x+d\}^{-4}. \quad (4.19)$$

At the same time one has to use Eq. (4.13) and the following integrals

$$\int d^4k(k^2-2p\cdot k-c)^{-4}=\frac{i\pi^2}{6}(p^2+c)^{-2},$$
$$\int d^4kk_\mu k_\nu(k^2-2p\cdot k-c)^{-4}=p_\mu p_\nu\frac{i\pi^2}{6}(p^2+c)^{-2}-g_{\mu\nu}\frac{\pi^2 i}{12(p^2+c)}. \quad (4.20)$$

After some laborious manipulations one arrives at

$$A_{3\mathrm{Ra}S}=-(2\pi)^{-6}G_1G_2B\left(\frac{m_1}{E_1}\right)^{1/2}\left(\frac{m_2}{E_2}\right)^{1/2}\left(\frac{1}{2K}\right)^{1/2}\left(\frac{1}{2Q}\right)^{1/2}e\delta(p_1-p_2-q-k)$$
$$\times i\tilde{W}^s(p_2)\{-(F_1+F_2m_2+F_3m_1-F_3m_2)\boldsymbol{k}(\gamma\cdot\epsilon^\lambda)-2F_3p_1\cdot k(\gamma\cdot\epsilon^\lambda)$$
$$-F_4p_2\cdot\epsilon^\lambda+F_5p_2\cdot\epsilon^\lambda+F_6p_2\cdot\epsilon^\lambda\boldsymbol{k}+F_7(\gamma\cdot\epsilon^\lambda)\}W^r(p_1), \quad (4.21)$$

where

$$F_1=\pi^2\int_0^1 dx\int_0^x dy\frac{-m}{2p_1\cdot k}\{\mu^2y^2+y[2p_2\cdot qx-(m_1^2-\mu^2-m_2^2+\mu_K^2-2p_1\cdot k)]+m_2^2x^2+m^2-(m_2^2-\mu_K^2+m^2)x\}^{-1},$$

$$F_2=\pi^2\int_0^1 dx\int_0^x dy\frac{x}{2p_1\cdot k}\{\mu^2y^2+y[2p_2\cdot qx-(m_1^2-\mu^2-m_2^2+\mu_K^2-2p_1\cdot k)]+m_2^2x^2+m^2-(m_2^2-\mu_K^2+m^2)x\}^{-1},$$

$$F_3=\pi^2\int_0^1 dx\int_0^x dy\frac{y}{2p_1\cdot k}\{\mu^2y^2+y[2p_2\cdot qx-(m_1^2-\mu^2-m_2^2+\mu_K^2-2p_1\cdot k)]+m_2^2x^2+m^2-(m_2^2-\mu_K^2+m^2)x\}^{-1},$$

$$F_4=-\pi^2\frac{1}{q\cdot k}\int_0^1 dx\int_0^x dy(m_1y-m_2y+m_2x-m)\{y^2(m_1^2+m_2^2-2p_1\cdot p_2)$$
$$+y[2p_1\cdot px-2m_2^2x-(m_1^2-\mu^2-m_2^2+\mu_2^2)]+m_2^2x^2-(m_2^2-\mu_2^2+m^2)x+m^2\},$$

$$F_5=-\pi^2\int_0^1 dx\int_0^x dy\int_0^y dz\,2(x-y)(m_1y-m_2y+m_2x-m)\frac{1}{DE^2},$$

$$F_6=\pi^2\int_0^1 dx\int_0^x dy\int_0^y dz\,2(x-y)z\frac{1}{DE^2},$$

$$F_7=\pi^2\int_0^1 dx\int_0^x dy\int_0^y dz\frac{1}{DE}, \quad (4.22)$$

and

$$DE=(-zk+p_1y-p_2y+p_2x)^2+2p_1\cdot kz+m^2-(m_1^2-\mu^2-m_2^2+\mu_K^2)y-(m_2^2-\mu_K^2+m^2)x. \quad (4.23)$$

Equation (4.21) has a form similar to those of Eq. (4.7) and Eq. (4.10), so we can use the same steps to find the expression of the transition probability for this virtual $\bar{K}^0$-meson loop as in the pole cases. The amplitude $A_{3\mathrm{Ra}S}$ as given by Eq. (4.23) is already in a good form for numerical calculation. The numerical results are presented in Sec. V.

V. DISCUSSION

All numerical results for the preceding models are presented in the tables and figures of this section. The results of our calculations indicate that the spectra for s- and p-wave decay are distinctly different in all the models. Except for the model with a virtual K-meson loop, all other models give similar s-wave and p-wave spectra. The slight difference between the spectra for either wave found for the different models may be accounted for by the variations in magnetic corrections. The contributions to the decay spectrum from the virtual K-meson loop model is found to be very small. Thus it may be ignored.

The current terms in a simple phenomenological model and in all pole models are the same. This is the main term that distinguishes between s and p wave for the radiative decays. The magnetic term only provides a correction to this main term. Although we have considered each of these models one at a time, the order of magnitude of the deviations from the first phenomenological model implies that the interferences between these model contributions, if they were treated simultaneously, would not change the main features. The

TABLE V. The differential and integral value of $W(\Sigma^+ \to n+\pi^+)$ as a function of pion momentum, q, for s wave $\Sigma^+ \to n+\pi^+$ decay, under the Σ^0 pole model.

$\lvert q\rvert$	Current contribution	Magnetic moment corrections $\mu_{\Sigma^+}=3.79$	$\mu_{\Sigma^+}=1.79$	$\mu_{\Sigma^+}=0.00$	$\mu_{\Sigma^+}=-1.79$	$\mu_{\Sigma^+}=-2.79$
			$\mu_{\Sigma^0}=1.79$			
20	0.29×10^{-7}	0.178×10^{-6}	0.96×10^{-7}	0.42×10^{-7}	0.71×10^{-8}	-0.99×10^{-8}
40	0.72×10^{-6}	0.145×10^{-5}	0.77×10^{-6}	0.33×10^{-6}	0.45×10^{-7}	-0.89×10^{-7}
60	0.51×10^{-5}	0.48×10^{-5}	0.252×10^{-5}	0.104×10^{-5}	0.102×10^{-6}	-0.32×10^{-6}
80	0.21×10^{-4}	0.109×10^{-4}	0.56×10^{-5}	0.225×10^{-5}	0.102×10^{-6}	-0.82×10^{-6}
100	0.67×10^{-4}	0.202×10^{-4}	0.102×10^{-5}	0.393×10^{-5}	-0.37×10^{-7}	-0.163×10^{-5}
120	0.174×10^{-3}	0.324×10^{-4}	0.162×10^{-4}	0.59×10^{-5}	-0.35×10^{-6}	-0.271×10^{-5}
140	0.41×10^{-3}	0.46×10^{-4}	0.230×10^{-4}	0.81×10^{-5}	-0.82×10^{-6}	-0.393×10^{-5}
160	0.99×10^{-3}	0.60×10^{-4}	0.296×10^{-4}	0.102×10^{-4}	-0.131×10^{-5}	-0.501×10^{-5}
180	0.32×10^{-2}	0.69×10^{-4}	0.33×10^{-4}	0.118×10^{-4}	-0.161×10^{-5}	-0.56×10^{-5}
			$\mu_{\Sigma^0}=0.00$			
20	0.29×10^{-7}	0.172×10^{-6}	0.91×10^{-7}	0.39×10^{-7}	0.46×10^{-8}	-0.114×10^{-7}
40	0.72×10^{-6}	0.138×10^{-5}	0.71×10^{-6}	0.278×10^{-6}	-0.74×10^{-9}	-0.127×10^{-6}
60	0.51×10^{-5}	0.44×10^{-5}	0.218×10^{-5}	0.73×10^{-6}	-0.185×10^{-6}	-0.58×10^{-6}
80	0.21×10^{-4}	0.98×10^{-5}	0.45×10^{-5}	0.212×10^{-5}	-0.88×10^{-6}	-0.174×10^{-5}
100	0.67×10^{-4}	0.175×10^{-4}	0.76×10^{-5}	0.143×10^{-5}	-0.243×10^{-5}	-0.39×10^{-5}
120	0.174×10^{-3}	0.273×10^{-4}	0.113×10^{-4}	0.122×10^{-5}	-0.49×10^{-5}	-0.71×10^{-5}
140	0.41×10^{-3}	0.38×10^{-4}	0.153×10^{-4}	0.64×10^{-6}	-0.81×10^{-5}	-0.110×10^{-4}
160	0.99×10^{-3}	0.49×10^{-4}	0.190×10^{-4}	-0.213×10^{-7}	-0.112×10^{-4}	-0.147×10^{-4}
180	0.32×10^{-2}	0.56×10^{-4}	0.213×10^{-4}	-0.40×10^{-6}	-0.132×10^{-4}	-0.169×10^{-4}
			$\mu_{\Sigma^0}=-1.79$			
20	0.29×10^{-7}	0.167×10^{-6}	0.87×10^{-7}	0.36×10^{-7}	0.240×10^{-8}	-0.126×10^{-7}
40	0.72×10^{-6}	0.131×10^{-5}	0.65×10^{-6}	0.23×10^{-6}	-0.44×10^{-7}	-0.162×10^{-6}
60	0.51×10^{-5}	0.409×10^{-5}	0.187×10^{-5}	0.45×10^{-6}	-0.45×10^{-6}	-0.82×10^{-6}
80	0.21×10^{-4}	0.86×10^{-5}	0.353×10^{-5}	0.25×10^{-6}	-0.179×10^{-5}	-0.258×10^{-5}
100	0.67×10^{-4}	0.149×10^{-4}	0.52×10^{-5}	-0.91×10^{-6}	-0.47×10^{-5}	-0.60×10^{-5}
120	0.174×10^{-3}	0.225×10^{-4}	0.67×10^{-5}	-0.33×10^{-5}	-0.93×10^{-5}	-0.112×10^{-4}
140	0.41×10^{-3}	0.309×10^{-4}	0.78×10^{-5}	-0.66×10^{-5}	-0.151×10^{-4}	-0.177×10^{-4}
160	0.99×10^{-3}	0.39×10^{-4}	0.88×10^{-5}	-0.99×10^{-5}	-0.209×10^{-4}	-0.240×10^{-4}
180	0.32×10^{-2}	0.44×10^{-4}	0.93×10^{-5}	-0.119×10^{-4}	-0.245×10^{-4}	-0.279×10^{-4}

magnetic terms can become larger as one progresses from the simple phenomenological model to the proton-pole or $\Sigma^0(\Lambda)$-pole model, depending on one's choice of magnetic moments.

In Table V and Figs. 11 and 12 we display the numerical results for Σ^+ decays, using the proton-pole model of Sec. IV. The current term contribution is identical to the previous model of Sec. III, and the magnetic moment contribution has the same form but is slightly larger for corresponding value of μ_{K^+}. Tables VI and VII contain the numerical results for Σ^+ decays using the $\Sigma^0(\Lambda)$ pole model. The range of values for the magnetic moment terms is somewhat larger since we have two unknown magnetic moment terms to select, but in any case they remain small compared to the dominant current term. Table VIII gives the contribution from the K-loop diagram of Sec. IV, which turns out to be completely negligible. Figure 13 displays the s- and p-wave predictions for $\Sigma^+ \to n+\pi^++\gamma$ decays for the maximal magnetic moment contribution ($\mu_{\Sigma^+}=3.79$) in the "proton model." It is clear from the figure, that the essential point of Nauenberg *et al.*,[1] namely that p-wave decay is significantly larger than s-wave decay, remains a common feature of all the models considered.

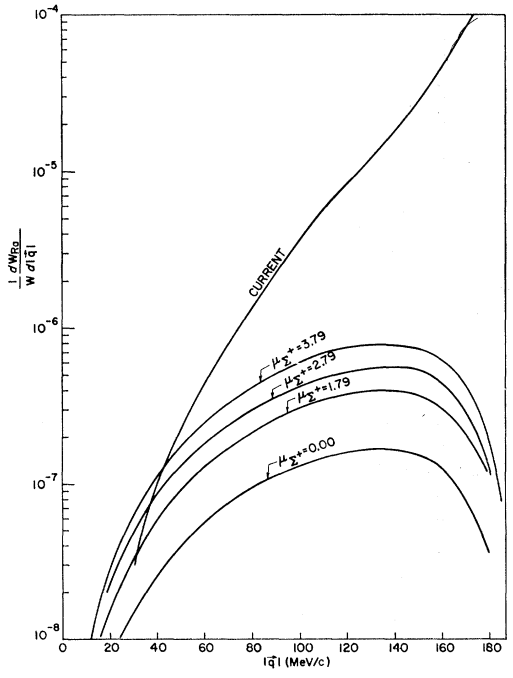

FIG. 11. The differential value $W(\Sigma^+ \to n+\pi^++\gamma)/W(\Sigma^+ \to n+\pi^+)$ and its magnetic correction as a function of the pion momentum $|q|$, for s wave in the proton pole model.

TABLE VI. The differential and integral value of $W(\Sigma^+ \to n+\pi+\gamma)/W(\Sigma^+ \to n+\pi^+)$ as a function of pion momentum, q, for p wave $\Sigma^+ \to n+\pi^+$ decay under the Σ^0 pole model.

$\|q\|$	Current contribution	Magnetic moment corrections $\mu_{\Sigma^+}=3.79$	$\mu_{\Sigma^+}=1.79$	$\mu_{\Sigma^+}=0.00$	$\mu_{\Sigma^+}=-1.79$	$\mu_{\Sigma^+}=-2.79$
			$\mu_{\Sigma^0}=1.79$			
20	0.110×10^{-5}	0.42×10^{-7}	0.280×10^{-7}	0.158×10^{-7}	0.43×10^{-8}	-0.81×10^{-8}
40	0.92×10^{-5}	0.40×10^{-6}	0.32×10^{-6}	0.258×10^{-6}	0.207×10^{-6}	0.165×10^{-6}
60	0.32×10^{-4}	0.161×10^{-5}	0.147×10^{-5}	0.143×10^{-5}	0.148×10^{-5}	0.165×10^{-5}
80	0.80×10^{-4}	0.42×10^{-5}	0.43×10^{-5}	0.46×10^{-5}	0.54×10^{-5}	0.65×10^{-5}
100	0.168×10^{-3}	0.84×10^{-5}	0.92×10^{-5}	0.108×10^{-4}	0.132×10^{-4}	0.170×10^{-4}
120	0.32×10^{-3}	0.137×10^{-4}	0.158×10^{-4}	0.197×10^{-4}	0.254×10^{-4}	0.34×10^{-4}
140	0.61×10^{-3}	0.190×10^{-4}	0.232×10^{-4}	0.303×10^{-4}	0.41×10^{-4}	0.56×10^{-4}
160	0.123×10^{-2}	0.232×10^{-4}	0.294×10^{-4}	0.401×10^{-4}	0.55×10^{-4}	0.78×10^{-4}
180	0.34×10^{-2}	0.252×10^{-4}	0.33×10^{-4}	0.46×10^{-4}	0.65×10^{-4}	0.92×10^{-4}
			$\mu_{\Sigma^0}=0.00$			
20	0.110×10^{-5}	0.35×10^{-5}	-0.24×10^{-5}	-0.78×10^{-5}	-0.131×10^{-4}	-0.191×10^{-4}
40	0.92×10^{-5}	0.38×10^{-5}	-0.23×10^{-5}	-0.76×10^{-5}	-0.131×10^{-4}	-0.191×10^{-4}
60	0.32×10^{-4}	0.45×10^{-5}	-0.160×10^{-5}	-0.69×10^{-5}	-0.123×10^{-4}	-0.181×10^{-4}
80	0.80×10^{-4}	0.60×10^{-5}	0.92×10^{-5}	-0.49×10^{-5}	-0.960×10^{-5}	-0.144×10^{-4}
100	0.168×10^{-3}	0.85×10^{-5}	0.32×10^{-5}	-0.66×10^{-6}	-0.37×10^{-5}	-0.59×10^{-5}
120	0.32×10^{-3}	0.117×10^{-4}	0.77×10^{-5}	0.59×10^{-5}	$+0.61\times10^{-5}$	0.84×10^{-5}
140	0.61×10^{-3}	0.151×10^{-4}	0.128×10^{-4}	0.143×10^{-4}	0.189×10^{-4}	0.28×10^{-4}
160	0.123×10^{-2}	0.178×10^{-4}	0.175×10^{-4}	0.224×10^{-4}	0.32×10^{-4}	0.48×10^{-4}
180	0.34×10^{-2}	0.192×10^{-4}	0.202×10^{-4}	0.274×10^{-4}	0.40×10^{-4}	0.62×10^{-4}
			$\mu_{\Sigma^0}=-1.79$			
20	0.110×10^{-5}	0.147×10^{-7}	0.77×10^{-9}	-0.112×10^{-7}	-0.229×10^{-7}	-0.35×10^{-7}
40	0.92×10^{-5}	0.124×10^{-6}	0.35×10^{-7}	-0.32×10^{-7}	-0.87×10^{-7}	-0.135×10^{-6}
60	0.32×10^{-4}	0.43×10^{-6}	0.25×10^{-6}	0.186×10^{-6}	0.20×10^{-6}	0.32×10^{-6}
80	0.80×10^{-4}	0.102×10^{-5}	0.94×10^{-6}	0.121×10^{-5}	0.180×10^{-5}	0.28×10^{-5}
100	0.168×10^{-3}	0.193×10^{-5}	0.24×10^{-5}	0.37×10^{-5}	0.59×10^{-5}	0.94×10^{-5}
120	0.32×10^{-3}	0.31×10^{-5}	0.47×10^{-5}	0.81×10^{-5}	0.133×10^{-4}	0.21×10^{-4}
140	0.61×10^{-3}	0.45×10^{-5}	0.78×10^{-5}	0.142×10^{-4}	0.24×10^{-4}	0.38×10^{-4}
160	0.123×10^{-2}	0.59×10^{-5}	0.110×10^{-4}	0.21×10^{-4}	0.35×10^{-4}	0.57×10^{-4}
180	0.34×10^{-2}	0.68×10^{-5}	0.132×10^{-4}	0.25×10^{-4}	0.43×10^{-4}	0.70×10^{-4}

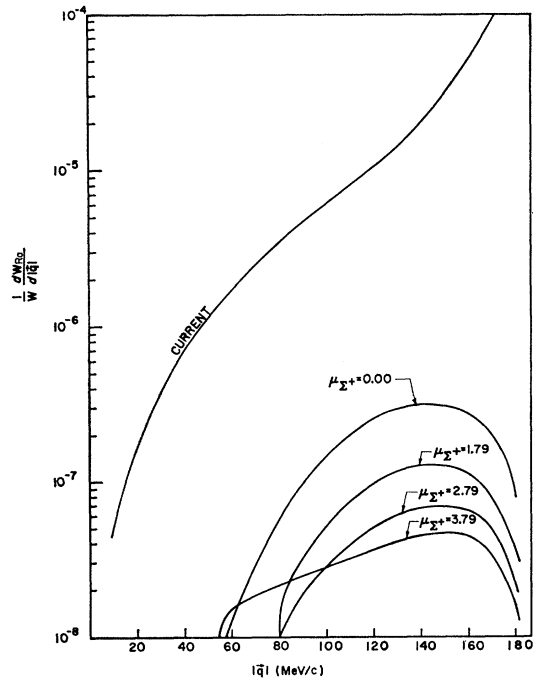

FIG. 12. The differential value $W(\Sigma^+ \to n+\pi^++\gamma)/W(\Sigma^+ \to n+\pi^+)$ and its magnetic correction as a function of the pion momentum $|q|$, for p wave in the proton pole model.

The advantage of the pole models is that they give us a natural way to include the weak vertices $\Sigma^+ \to p+\gamma$, $\Sigma^0 \to n+\gamma$, and $\Lambda^0 \to n+\gamma$. These vertices can only be taken into account in a phenomenological model by introducing a "transition" magnetic moment artificially. Actually, understanding the possible contribution of these weak vertices to the radiative pionic decay transition is essential before one can have confidence in the previous calculations. As Dosch[8] has pointed out to us, if the $\Sigma^+ \to p+\gamma$ transition has the following vertex form:

$$\bar{U}(p)\{(p+\Sigma)\cdot K\gamma\cdot\epsilon-(p+\Sigma)\cdot\epsilon K\}U(\Sigma), \quad (5.1)$$

where p, Σ, K are the momenta of the proton, Σ-hyperon, and photon, and ϵ is the polarization vector of the photon [$\bar{U}(p)$, $U(\Sigma)$ are the corresponding spinors], then the contribution from this vertex in the Σ-radiative decay is comparable with the *current* term. The important point is that the pole models enable us to predict the $\Sigma^+ \to p+\gamma$ transition without giving rise to terms like (5.1) that would drastically change the rate in the radiative-decay calculations. Hence the pole models

[8] H. G. Dosch (private communication).

TABLE VII. The differential and integral value of $W(\Sigma^+ \to n+\pi^+)$ as a function of the pion momentum, q, under the virtual K-meson loop.

$\|q\|$	Differential	Integral
30	0.25×10^{-8}	0.24×10^{-7}
60	0.133×10^{-7}	0.23×10^{-6}
90	0.452×10^{-7}	0.102×10^{-5}
120	0.140×10^{-6}	0.354×10^{-5}
140	0.303×10^{-6}	0.80×10^{-5}
160	0.49×10^{-6}	0.117×10^{-4}
180	0.59×10^{-5}	0.60×10^{-4}

provide a self-consistent model for the radiative pionic and nonpionic decays.

The negligibly small contribution of the virtual K-meson loop indicates that the inner bremsstrahlung from the virtual swift light particle can be discarded. *A priori*, one generally believes that the faster a charged particle moves, the greater its contribution will be to the inner bremsstrahlung. Then one might conjecture that high-energy intermediate states that affect the hyperon-proton form factor might contribute significantly to the radiative decays. The loop-model calculation, if it can be taken as a prototype of such form factor effects, indicates that despite the general conjecture, these intermediate states will not contribute significantly to radiative decays.

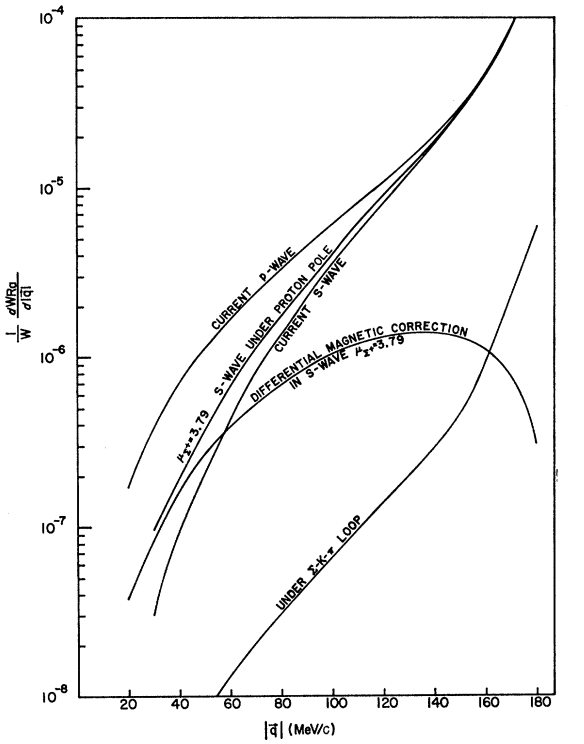

FIG. 13. The s- and p-wave predictions for $\Sigma^+ \to n+\pi^++\gamma$ decays for the maximal magnetic moment contribution ($\mu_{\Sigma^+}=3.79$) in the proton pole model. In comparison the virtual K-meson contribution is also listed.

TABLE VIII. In samples of 14 800 $\Sigma^+ \to n+\pi^+$ and 25 000 $\Sigma^- \to n+\pi^-$ the events found for the radiative decays $\Sigma^{\pm} \to n+\pi^{\pm}+\gamma$ are listed in the second column of each table. The data are copied from Nauenberg *et al.* The experimental branch ratios are the ratios between these observed events and the number of samples. The theoretical branch ratios are the current contribution to the integral values of $W(\Sigma^{\pm} \to n+\pi^{\pm}+\gamma)/W(\Sigma^{\pm} \to n+\pi^{\pm})$. As we said in the text, the current contribution is the main term and is the same for the phenomenological and pole models.

A sample of 14 800 $\Sigma^+ \to n+\pi^+$

$\|q\|$	Observed events for $\Sigma^+ \to n+\pi^++\gamma$	Experimental branching ratio	Theoretical branching ratio s wave	p wave
80	1	0.67×10^{-4}	0.21×10^{-4}	0.80×10^{-4}
100	4	0.27×10^{-3}	0.67×10^{-4}	0.168×10^{-3}
120	7.5	0.506×10^{-3}	0.174×10^{-3}	0.32×10^{-3}
140	11.5	0.84×10^{-3}	0.41×10^{-3}	0.61×10^{-3}
160	22.5	1.52×10^{-3}	0.99×10^{-3}	1.23×10^{-3}
165	24.0	1.62×10^{-3}	1.28×10^{-3}	1.53×10^{-3}

A sample of 25 000 $\Sigma^- \to n+\pi^+$

$\|q\|$	Observed events for $\Sigma^- \to n+\pi^-+\gamma$	Experimental branching ratio	Theoretical branching ratio s wave	p wave
80	0	0	0.19×10^{-4}	0.75×10^{-4}
100	1	0.4×10^{-4}	0.58×10^{-4}	0.155×10^{-3}
120	5	0.2×10^{-3}	0.15×10^{-3}	0.30×10^{-3}
140	11	0.44×10^{-3}	0.35×10^{-3}	0.55×10^{-3}
160	23	0.92×10^{-3}	0.79×10^{-3}	1.04×10^{-3}
165	26.5	1.06×10^{-3}	1.00×10^{-3}	1.25×10^{-3}

An experiment on radiative $\Sigma^{\pm}$ decays has been carried out by Nauenberg *et al.*[9] They studied a sample of 14 800 $\Sigma^+ \to n+\pi^+$ decays and a sample of 25 000 $\Sigma^- \to \pi^-+n$ decays. From these samples they found a number of radiative decay events for the different pion moments which are recopied in Table VIII. From these data, one can calculate the experimental branch ratio. For comparison we also list theoretical values which are calculated from the current contribution of the phenomenological and the pole models. In the case of $\Sigma^+ \to \pi^++n+\gamma$ decay the experimental branching ratio is bigger than the theoretical values. If we take into account the magnetic corrections and the experimental errors, the results strongly indicate p wave for the $\Sigma^+ \to \pi^++n$ decay. In the other case $\Sigma^- \to \pi^-+n+\gamma$ the experimental ratio lies between the theoretical values. Even if we take into account the magnetic corrections and the experimental errors, it is difficult to choose between the p-wave or s-wave

[9] U. Nauenberg, M. Bazin, H. Blumenfeld, L. Seidlitz, S. Marateck, R. J. Plano, and P. Smith, Phys. Rev. **140**, B1358 (1965).

hypotheses for the $\Sigma^- \to n+\pi^-$ decay. Nevertheless, if one assumes the $\Delta I=\frac{1}{2}$ rule and the experimentally measured asymmetry parameter values, the experimental results of the radiative hyperon decays strongly favor the assignment $\Sigma^+ \to \pi^+ + n$ (p wave) and $\Sigma^- \to \pi^- + n$ (s wave), rather than the reverse.

ACKNOWLEDGMENT

The author is grateful to Dr. George A. Snow for having suggested this problem and for his continued advice and encouragement. Also the author is indebted to Dr. U. Nauenberg for the experimental data cited in this paper and to Dr. H. G. Dosch for his comments.

PHYSICAL REVIEW VOLUME 141, NUMBER 4 JANUARY 1966

Consequences of C-Violating Interactions in η^0 and X^0 Decays*

BARBARA BARRETT
Department of Physics, Columbia University, New York, New York

MAURICE JACOB†
Stanford Linear Accelerator Center, Stanford University, Stanford, California

MICHAEL NAUENBERG‡
Stanford Linear Accelerator Center, Stanford University, Stanford, California

AND

TRAN N. TRUONG
Stanford Linear Accelerator Center, Stanford University, Stanford, California
and
Department of Physics, Brown University, Providence, Rhode Island

(Received 6 August 1965)

In this article several decay modes of the η and the X^0 (heavy η) meson are discussed under the assumption that there exist C-violating interactions which conserve parity and strangeness. Various speculations about the strength, symmetry, and electromagnetic properties of this interaction are considered to find out how these properties might be determined experimentally from these decays. From available experimental data, several limits for the strength of C-violating interactions are obtained.

INTRODUCTION

SINCE the discovery of the $\pi^+\pi^-$ decay mode of the long-lived neutral K meson,[1–3] there has been a great deal of speculation concerning the nature of the interaction which is responsible for this CP-violating transition. It has been pointed out recently[4–6] that a possible explanation is the existence of an interaction H which violates charge conjugation C, but conserves parity P and strangeness. The 2π decay of the K_2^0 occurs then as a second-order process in $H \times H_W$, where H_W is the CP-conserving $\Delta S=1$ weak interaction. The strength of H which accounts for the observed $K_2^0 \to 2\pi$ branching ratio is estimated to be of the order of electromagnetic interactions, but there is some uncertainty in this result because of the difficulties in calculating higher order processes.

The transformation properties under isospin and unitary spin of the C-violating interaction H are open to conjecture. It has been suggested that (a) H might correspond to the same interaction that is responsible for the breakdown of SU_3 symmetry which transforms like the $T=0$, $Y=0$ member of the octet[4]; (b) H may be part of the electromagnetic interaction of strongly interacting particles.[7,8] A number of experiments have been proposed to test the existence of H and examine its properties.[4–15]

* Work supported in part by the U. S. Atomic Energy Commission.

† Present address: Service de Physique Théorique, CEN Saclay, BP No. 2, Gif-sur-Yvette (Seine et Oise), France.

‡ A. P. Sloan Fellow.

[1] J. H. Christenson, J. W. Cronin, V. L. Fitch, and R. Turlay, Phys. Rev. Letters **13**, 138 (1964).

[2] V. L. Fitch, R. F. Roth, J. S. Russ, and W. Vernon, Phys. Rev. Letters **15**, 73 (1965).

[3] X. de Bouard *et al.*, Phys. Letters **15**, 58 (1965).

[4] L. Okun, Institute of Theoretical and Experimental Physics, Moscow (unpublished).

[5] J. Prenkti and M. Veltman, Phys. Letters **15**, 88 (1965).

[6] T. D. Lee and L. Wolfenstein, Phys. Rev. **138**, B1490 (1965).

[7] J. Bernstein, G. Feinberg, and T. D. Lee, Phys. Rev. **139**, B1650 (1965).

[8] S. Barshay, Phys. Letters **17**, 78 (1965).

[9] Y. Fujii and G. Marx, Phys. Letters **17**, 75 (1965).

[10] S. Glashow and C. Sommerfield, Phys. Rev. Letters **15**, 78 (1965).

[11] R. Friedberg, T. D. Lee, and M. Schwartz (see footnote 8 in Ref. 6).

[12] J. Prenkti and M. Veltman, Phys. Letters **17**, 77 (1965).

[13] This approximation neglects the energy dependence of the ρ width (see Sec. II).

[14] M. Nauenberg, Phys. Letters **17**, 329 (1965).

[15] T. D. Lee, Phys. Rev. **139**, B1415 (1965).